Discipline of Chemical Engineering
School of Engineering, Faculty of Engineering & Built Environment
The University of Newcastle, University Drive, Callaghan, NSW 2308, Australia

Technical Assessment of the Otello Heat Engine

FINAL REPORT

Performance Characteristics of the Otello Heat Engine Using R245fa, R410a, and CO_2 Working Fluids

Prepared by:

Dr Elham Doroodchi
Prof Behdad Moghtaderi

Date: 27 May, 2010

Report Prepared for the International Innovation Limited (IIL)

Disclaimer

The conclusions and recommendations presented in this report are solely based on theoretical predictions made using a mathematical model of the Otello heat engine. The model has been developed by authors using the information provided and constrains setup by IIL in 2009 and, hence, is only applicable to working fluids R245fa, R410a and CO_2 and source temperatures between 80^oC and 200^oC. Simplified assumptions were made in the development of the model particularly with regards to heat loss processes. Therefore, without further refinement of the model through a series of experimental validations, the model predictions should be merely considered as a guide. The authors strongly advise against the use of the model outside the framework described in this disclaimer and will not be liable for any predictions/conclusions resulting from such misuses.

TABLE OF CONTENTS

Page

Discipline of Chemical Engineering
School of Engineering, Faculty of Engineering & Built Environment
The University of Newcastle, University Drive, Callaghan, NSW 2308, Australia

1. BACKGROUND AND SUMMARY

The University of Newcastle was sub-contracted in early 2009 to assess the technical feasibility of the Otello heat engine developed by the International Innovation Limited (IIL). The work plan comprised:

- Stage 1- Development of an analysis tool based on thermodynamic and heat transfer principles.
- Stage 2- Case studies for 1 MW Otello plant.
- Stage 3- Preparation and dissemination of milestone reports.

The scope of the technical assessment for case studies associated with Stage 2 was limited to:

- working fluids: R245fa, R410a, and carbon dioxide (CO_2), and;
- initially heat source temperatures of 150^oC, 72^oC, and 31.5^oC although the range of source temperatures of interest was changed to 80^oC-200^oC after the submission of the interim report in Sept, 2009.

The report presented here builds upon the interim report submitted on 7th Sept, 2009 and provides:

- An overview of the analysis tool developed by the authors for mathematical description of the Otello heat engine.
- A technical assessment of the performance characteristics of the Otello heat engine when working fluids R245fa, R410a, and CO_2 are employed.

As detailed in the following sections among the three working fluids studied in the present investigation, R245fa exhibited the best performance in terms of performance indicators such as thermal efficiency, number of accumulators for a given output, and the overall frequency of the cycle. It was found that the Otello engine in conjunction with R245fa as a working fluid could attain a theoretical thermal efficiency of 13.7% at a source temperature of 200^oC and an ambient temperature of 25^oC using a series of 30 L accumulator units. Under these conditions the bench-mark Carnot efficiency is about 37%. The corresponding thermal efficiencies of R410a and CO_2 were 12.2% and 8%, respectively. The required numbers of accumulator units for R410a and CO_2 to attain the above thermal efficiencies were 4.5 and 38.3 times greater than that of the R245fa, highlighting the attractiveness of R245fa as a working fluid.

2. THE UNIVERSITY OF NEWCASTLE (UoN) ANALYSIS TOOL

2.1 Conceptual Framework of the UoN Analysis Tool

The development process for the UoN analysis tool initially began by examining the suitability of commercially available process simulation software packages such as HYSYS and CyclePad for modelling of the Otello heat engine. None of these commercial packages were found to be suitable and as such it was decided to develop a dedicated analysis tool for the Otello system which:

- Considers a fixed mass of the working fluid within the accumulator cylinder during major processes associated with the Otello thermodynamic cycle.
- Takes into account both thermodynamic and heat transfer issues.
- Robust enough to model both piston and bladder type accumulator cylinders systems.

The sub-processes considered in this study for the Otello heat engine thermodynamic cycle are schematically illustrated in Figure 1. The corresponding cycle on the temperature-entropy (T-S) diagram is shown in Figure 2.

As can be seen from Figures 1 and 2, the Otello thermodynamic cycle in the UoN model begins with pumping the working fluid from the saturated liquid State 1 to sub-cooled liquid State 2. The heat addition phase then commences. The energy added to the Otello system during the heat addition phase originates from a heat source. Rather than direct heat exchange between the source and the accumulator cylinder, the thermal energy of the source is used to heat a bath of water or oil in which the accumulator cylinders are placed. The heat addition process initially takes place between States 2 and 3 under constant pressure where as shown in Figure 1 the working fluid experiences some slight expansion. Once the working fluid reaches the saturated vapour State 3 the heat addition process continues under constant volume. As a result, the pressure and temperature of the working fluid rise until they reach their maximum values at the superheated State 4. The working fluid is then isentropically expanded to State 5. The volume of the working fluid during the expansion phase increases dramatically causing the piston (or bladder) to move, in turn, forcing the hydraulic liquid out of the accumulator generating mechanical work. Upon full expansion, the process of heat rejection to a cooling medium begins at constant pressure (between States 5 and 1) and the cycle comes to completion once the working fluid reaches State 1. The sub-processes described above are then repeated.

It should be noted that the T-S diagram shown in Figure 2 suggests that the Otello heat engine can be operated at temperatures higher than the critical temperature of the working fluid provided that the maximum cycle pressure is maintained at levels below the critical pressure.

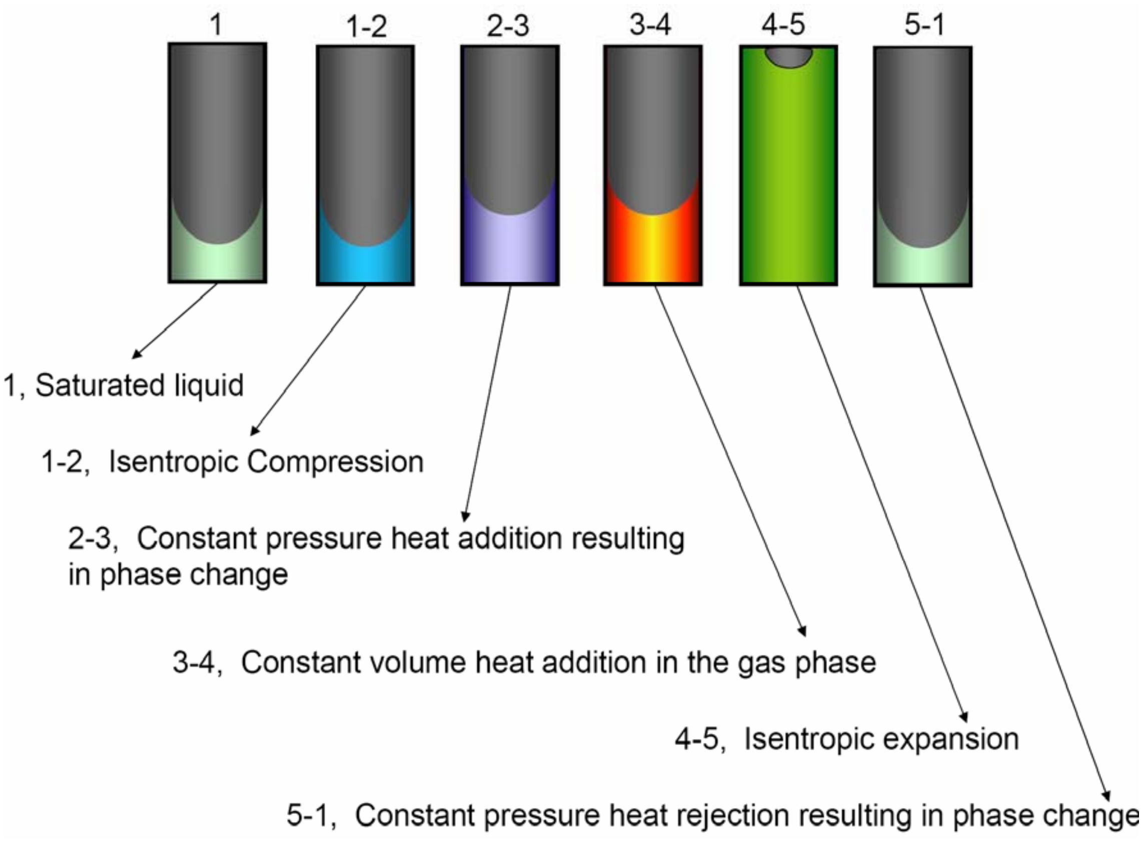

Figure 1: Schematic of the Otello heat engine sub-processes.

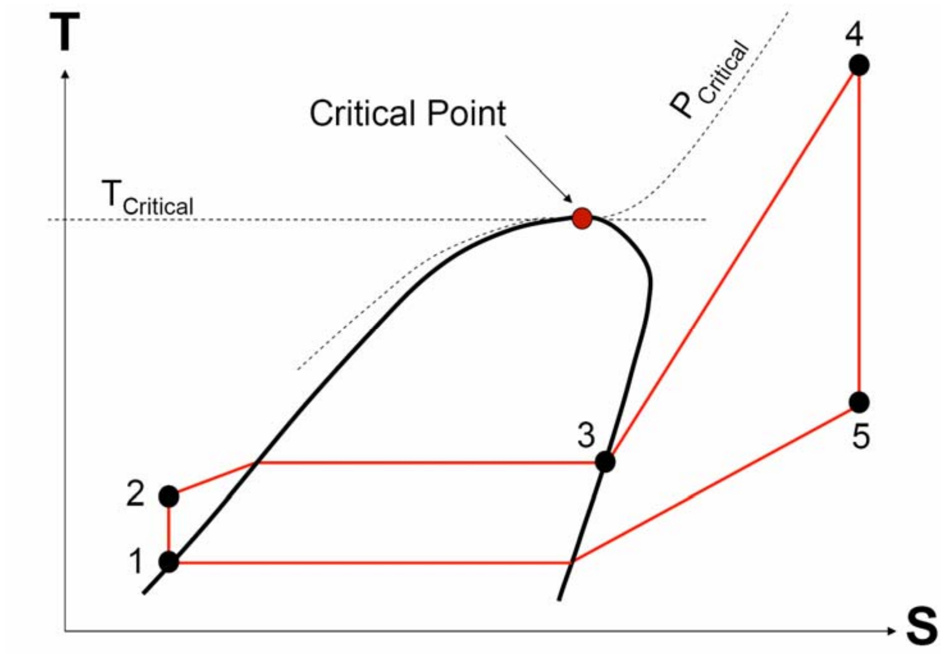

Figure 2: Schematic representation of the Otello heat engine on a T-S diagram.

2.2 Calculation Methodology

In terms of the solution methodology, the UoN analysis tool carries out two sets of simultaneous calculations, namely: energy balance (thermodynamic) and heat transfer. While the total energy exchanged during a given cycle is determined through the energy balance calculations based on thermodynamic principles, heat transfer calculations allow the transient behaviour of the Otello heat engine to be uncovered. Essentially the heat transfer calculations can tell us how long it would take for the thermal energy of the heat source to be transported to the working fluid inside the accumulator cylinder. This, in turn, allows us to accurately determine the period of a full cycle, the frequency of the system (e.g. revolution per minute, RPM), and the required number of accumulator cylinders to achieve a desired power output. Other performance characteristics of the engine, such as the thermal efficiency and the net power output can be determined from the energy balance calculations. The energy balance for the accumulator cylinder in the UoN analysis tool is carried out by determining the internal energy, entropy, density, temperature and pressure of the working fluid at States 1 to 5 from either input data or thermodynamic calculations. The heat transfer calculations are performed on the basis of the well known lumped parameter analysis. In these calculations the thermal resistance of the accumulator cylinder is ignored (this is just an approximation/simplification as in reality the cylinder walls act as barriers which slow down the transport of heat from the bath to the working fluid inside the accumulator). The flowchart of the overall calculation methodology is provided in Figure 3 while the major steps undertaken in lumped parameter analysis are given below.

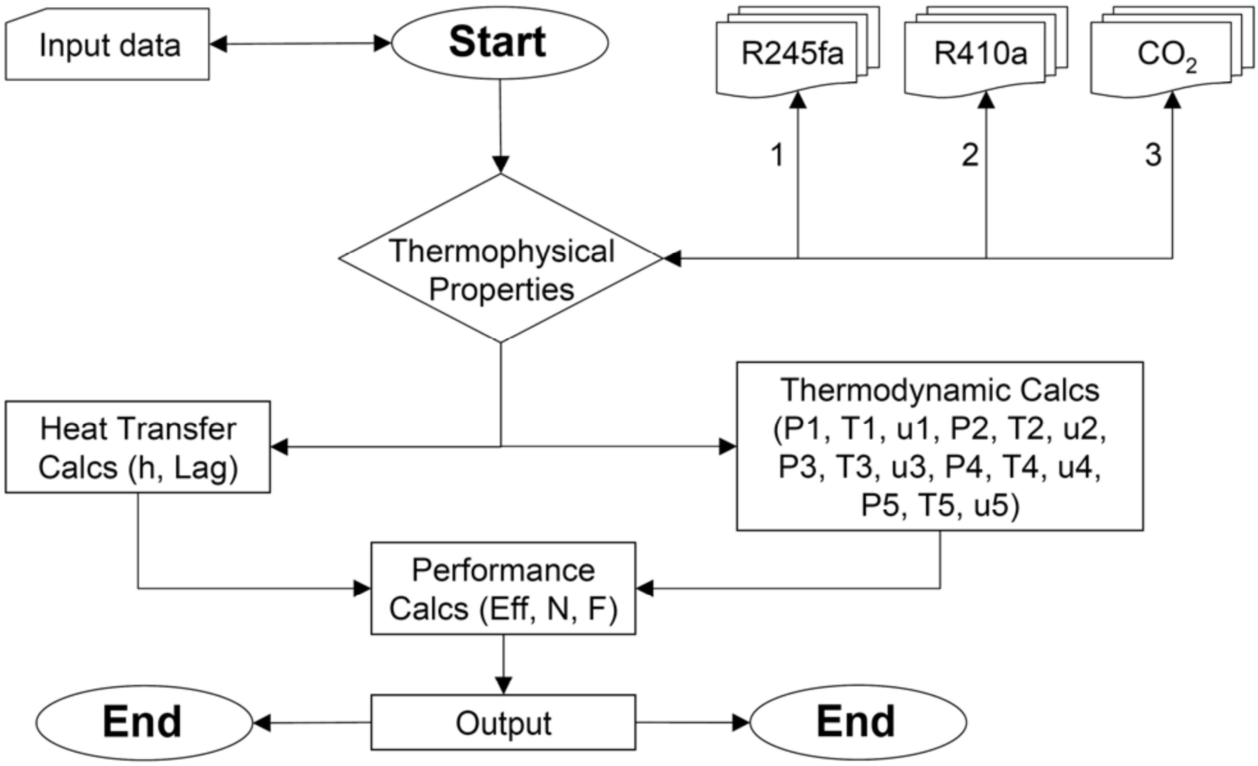

Figure 3: The flowchart of the calculation methodology.

<u>Details of lumped parameter analysis</u>

- Determination of bath convective heat transfer coefficient (h):
    - Read Prandtl number (Pr) and thermal conductivity (k_b) of the bath fluid from the input file
    - Determine Nassult number (Nu) from a relevant expression, for example: $Nu = 0.193 \times \mathrm{Re}^{0.618} \times \mathrm{Pr}^{0.33}$; where Re denotes the Reynolds number
    - Calculate h from: $h = (Nu \times k_b) / D$; where D is the diameter of the accumulator

- Determination the cycle period (t):
  - Determine the normalised temperature ratio (θ) from: $\theta = (T_f - T_b)/(T_0 - T_b)$; where T_f, T_b, and T_0 are the final, bath, and initial temperatures, respectively.
  - Determine the thermal lag (L_{ag}) from: $L_{ag} = \frac{hA}{\rho C_p V} = \frac{4h}{\rho C_p D}$; where ρ and C_p are the density and specific heats of the working fluid in the accumulator.
  - Determine the cycle period from: $t = \ln\left(\frac{\theta}{-L_{ag}}\right)$

3. RESULTS AND DISCUSSION

3.1 Summary of Findings from the Interim Report (R245fa only)

Eight case studies were carried out on R245fa as part of studies associated with interim report. Six case studies were dedicated to the source temperature 150^{o}C and accumulators of different volumes while two case studies were employed to the examine the relationships among the source temperature, maximum pressure and performance characteristics such as thermal efficiency, cycle frequency and the number of accumulator units. Special attention was given to the impact of the accumulator geometry and particularly its aspect ratio (*AR*) defined as the ratio of accumulator height to diameter (*H*/*D*).

It was found that for any given aspect ratio the cycle period was directly proportional to the accumulator capacity (i.e. volume). For example at *H*/*D* = 5.12 the cycle period for a 125 L accumulator was 216 s whereas that of the 2500 L accumulator was about 1597 s. The predicted cycle periods for all cases were greater than 200 s at aspect ratios below 10.

For typical accumulator cylinders currently available in the market with aspect ratios below 10, the frequency was determined to be about half revolution per minute for an accumulator with a capacity of 125 L. The frequency for larger capacity systems was typically lower than their small capacity counterparts reflecting the large thermal inertia of the Otello system. The corresponding number of accumulator units required to generate 1 MW of power for all case studies were calculated based on a combination of thermodynamic and heat transfer calculations. Analysis of different system configurations showed that the optimum combination was a system comprising a large number of small accumulators. This can be partly assigned to the fact that the rate of heat transfer and, hence, cycle period and frequency, are more favourable for a large number of smaller accumulators than a fewer number of medium (e.g. 1000 L) or large (e.g. 2500 L) accumulator cylinders.

The major conclusion from preliminary studies was that smaller accumulators with an aspect ratio of about 5 generally lead to improved performance characteristics. For case studies 1 to 6 the optimum combination for a source temperature of 150^{o}C was a system comprising 199 accumulators each with a capacity of 125 L and an aspect ratio of 5.12. The combined volume of the optimum system was approximately 25 m^3.

3.2 Performance Characteristics of Otello Heat Engine

Thirty new case studies were carried out as part of Milestone 2 to determine the operational envelope of a 1 MW Otello heat engine (see Tables 1 to 3). Case studies 1 to 10 were dedicated to R245fa while case studies 11-20 and 21-30 were devoted to R410a and CO_2, respectively. For each working fluid the accumulator capacity (i.e. volume) and source temperature were systematically changed to examine and compare the effects of accumulator size and source temperature on the performance characteristics of each working fluid. An ambient temperature of 25^{o}C was considered for R245fa and R410a. However, due to thermodynamic constrains the ambient temperature for CO_2 cases had to be lowered to levels about 20^{o}C, ensuring that CO_2 at point 1 of the cycle is in liquid form.

Based on the findings of the preliminary studies the aspect ratios of all accumulators studied were fixed at a nominal value of 5. Further, a 30 L accumulator was considered as the base configuration. In all case studies an approach temperature of 40^{o}C was maintained between the source (heat transfer medium in the bath for example water, thermal oil, etc) and the working fluid in the accumulator during the heat addition process. To maintain an optimised heat transfer between the source and working fluid, the heat transfer medium in the bath was assumed to be continuously stirred using a mechanical agitator. The Reynolds number of the flow induced by stirring was taken as 40,000.

Table 1: Input data for case studies 1 to 10 and corresponding operational parameters for R245fa

Parameter	Case Studies (R245fa)									
	1	**2**	**3**	**4**	**5**	**6**	**7**	**8**	**9**	**10**
Net power output (MW)	1	1	1	1	1	1	1	1	1	1
Accumulator capacity (L)	30	30	30	30	125	500	750	1000	2000	2500
Accumulator Diameter (mm)	197	197	197	197	317	503	576	634	799	861
Accumulator aspect ratio (H/D)	5	5	5	5	5	5	5	5	5	5
Volume Expansion (V_{max}/V_{min})	4	4	4	4	4	4	4	4	4	4
Source temperature (^{o}C)	120	150	175	200	200	200	200	200	200	200
Ambient temperature (^{o}C)	25	25	25	25	25	25	25	25	25	25
Minimum pressure (MPa)	0.2	0.2	0.2	0.2	0.2	0.2	0.2	0.2	0.2	0.2
* Re = 40,000	✓	✓	✓	✓	✓	✓	✓	✓	✓	✓

* *Re ≡ Reynolds number of the heat transfer medium (e.g. water, thermal oil, etc) in the bath.*

Table 2: Input data for case studies 11 to 20 and corresponding operational parameters for R410a

Parameter	Case Studies (R410a)									
	11	**12**	**13**	**14**	**15**	**16**	**17**	**18**	**19**	**20**
Net power output (MW)	1	1	1	1	1	1	1	1	1	1
Accumulator capacity (L)	30	30	30	30	125	500	750	1000	2000	2500
Accumulator Diameter (mm)	197	197	197	197	317	503	576	634	799	861
Accumulator aspect ratio (H/D)	5	5	5	5	5	5	5	5	5	5
Volume Expansion (V_{max}/V_{min})	4	4	4	4	4	4	4	4	4	4
Source temperature (^{o}C)	120	150	175	200	200	200	200	200	200	200
Ambient temperature (^{o}C)	25	25	25	25	25	25	25	25	25	25
Minimum pressure (MPa)	1.9	1.9	1.9	1.9	1.9	1.9	1.9	1.9	1.9	1.9
* Re = 40,000	✓	✓	✓	✓	✓	✓	✓	✓	✓	✓

* *Re ≡ Reynolds number of the heat transfer medium (e.g. water, thermal oil, etc) in the bath.*

Table 3: Input data for case studies 21 to 30 and corresponding operational parameters for CO_2

Parameter	Case Studies (CO_2)									
	21	**22**	**23**	**24**	**25**	**26**	**27**	**28**	**29**	**30**
Net power output (MW)	1	1	1	1	1	1	1	1	1	1
Accumulator capacity (L)	30	30	30	30	125	500	750	1000	2000	2500
Accumulator Diameter (mm)	197	197	197	197	317	503	576	634	799	861
Accumulator aspect ratio (H/D)	5	5	5	5	5	5	5	5	5	5
Volume Expansion (V_{max}/V_{min})	4	4	4	4	4	4	4	4	4	4
Source temperature (^oC)	120	150	175	200	200	200	200	200	200	200
Ambient temperature (^oC)	20	20	20	20	20	20	20	20	20	20
Minimum pressure (MPa)	6.5	6.5	6.5	6.5	6.5	6.5	6.5	6.5	6.5	6.5
* Re = 40,000	✓	✓	✓	✓	✓	✓	✓	✓	✓	✓

* *Re ≡ Reynolds number of the heat transfer medium (e.g. water, thermal oil, etc) in the bath.*

A summary of major results for each case study has been provided in Table 4 (see below). The results presented in Table 4 are discussed further in this section. Results of additional calculations requested by IIL for a range of other diameters are presented in Appendix B.

Table 4: Major results for case studies 1 to 30 assuming 1 MW net power (*continues on the next page*)

Parameter	Case Studies (R245fa), Ambient Temperature = 25^oC									
	1	**2**	**3**	**4**	**5**	**6**	**7**	**8**	**9**	**10**
Source temperature (^oC)	120	150	175	200	200	200	200	200	200	200
Accumulator Volume (L)	30	30	30	30	125	500	750	1000	2000	2500
Maximum pressure (MPa)	0.65	1.56	2.45	3.23	3.23	3.23	3.23	3.23	3.23	3.23
Cycle period (s)	59	97	150	239	619	1558	2043	2475	3926	4559
Cycle frequency (RPM)	1.01	0.62	0.40	0.25	0.10	0.04	0.03	0.02	0.018	0.013
Mass flow rate of R245fa per accumulator (kg/s)	9.9	9.9	9.9	9.9	41.3	165	248	330	660	825
Net power per accumulator unit (kW)	2.3	2.5	2.03	1.5	2.41	3.83	4.38	4.83	6.08	6.55
Number of accumulators	434	401	492	667	415	261	228	207	164	153
Thermal efficiency (%)	6.4	10.8	12.7	13.7	13.7	13.7	13.7	13.7	13.7	13.7

Parameter	Case Studies (R410a), Ambient Temperature = 25^{o}C									
	11	**12**	**13**	**14**	**15**	**16**	**17**	**18**	**19**	**20**
Source temperature (^{o}C)	120	150	175	200	200	200	200	200	200	200
Accumulator Volume (L)	30	30	30	30	125	500	750	1000	2000	2500
Maximum pressure (MPa)	2.8	4.5	6.6	9.6	9.6	9.6	9.6	9.6	9.6	9.6
Cycle period (s)	72	136	270	652	1688	4250	5572	6751	10709	12437
Cycle frequency (RPM)	0.83	0.44	0.22	0.09	0.04	0.02	0.01	0.009	0.006	0.005
Mass flow rate of R410a per accumulator (kg/s)	7.7	7.7	7.7	7.7	32.2	129	194	258	516	645
Net power per accumulator unit (kW)	0.72	0.90	0.65	0.33	0.53	0.84	0.97	1.06	1.34	1.44
Number of accumulators	1389	1107	1528	3027	1881	1184	1035	940	746	693
Thermal efficiency (%)	3.4	7.5	10.3	12.2	12.2	12.2	12.2	12.2	12.2	12.2
Parameter	**Case Studies (CO_2), Ambient Temperature = 20^{o}C**									
	21	**22**	**23**	**24**	**25**	**26**	**27**	**28**	**29**	**30**
Source temperature (^{o}C)	120	150	175	200	200	200	200	200	200	200
Accumulator Volume (L)	30	30	30	30	125	500	750	1000	2000	2500
Maximum pressure (MPa)	11.3	15.75	18.3	21.5	21.5	21.5	21.5	21.5	21.5	21.5
Cycle period (s)	423	1403	1508	2085	5398	13591	17822	21591	34249	39775
Cycle frequency (RPM)	0.16	0.04	0.039	0.029	0.01	0.004	0.0034	0.0028	0.0018	0.0015
Mass flow rate of CO_2 per accumulator (kg/s)	5.3	5.3	5.3	5.3	22	88	132	176	352	440
Net power per accumulator unit (kW)	0.002	0.02	0.037	0.04	0.06	0.10	0.11	0.13	0.16	0.17
Number of accumulators	475689	63749	26768	25553	15879	9995	8738	7940	6297	5850
Thermal efficiency (%)	0.1	2.8	6.2	8.0	8.0	8.0	8.0	8.0	8.0	8.0

Figure 4 illustrates plots of the period of a full cycle versus accumulator volume for R245fa, R410a, and CO_2, respectively. The results shown in this figure were obtained from case studies 4-10, 14-20, and 24-30.

As can be seen, all three working fluids exhibit very similar trends although in all cases the predicted cycle periods for R245fa is much lower than those corresponding to R410a and CO_2. On average the cycle periods associated with R410a are 2.7 times greater than values associated with R245fa while in the case of CO_2 the disparity is even higher with CO_2 cycle periods being almost 9 times greater than those of the R245fa.

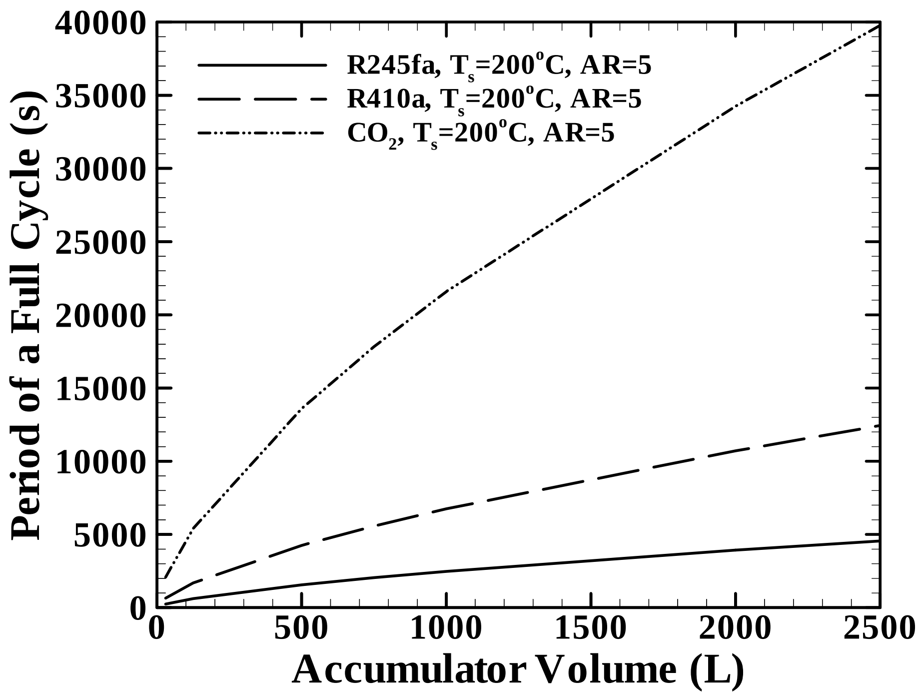

Figure 4: Cycle period versus accumulator volume for R245fa, R410a and CO_2.

The cycle frequencies (in revolution per minute, RPM) corresponding to cycle periods shown in Figure 4 have been summarised in Figure 5 and have been presented on a logarithmic scale for clarity. In each case the frequency has been calculated from: F = 60 × (1 / Period) and as such the cycle frequencies of R245fa are much higher than their R410a and CO_2 counterparts. Very much like the plots of cycle periods, the frequency plots shown in Figures 5 have almost identical trends although in terms of the absolute values they are vastly different. Higher frequencies are generally preferred because for a desired output (e.g. 1 MW) as they lead to a much smaller number of accumulator units and, thereby, significantly reduce the capital and maintenance costs. This is quite evident from Figure 6 where the number of required accumulators has been plotted on a logarithmic scale against the accumulator volume for R245fa, R410a and CO_2, respectively. Once again, the trends observed in all three figures are very similar to each other but the actual numbers quite different. Interestingly, the trends observed in Figure 6 are also similar to those observed earlier in Figure 5 primarily because of the direct relationship between the cycle frequency and accumulator numbers.

Given the importance of small accumulators in terms of shorter cycle periods, higher frequencies and smaller number of required units, the performance characteristics of R245fa, R410a, and CO_2 were compared in a 30 L accumulator unit at a source temperature of 200°C (i.e. case studies 4, 14, 24). The results of these comparisons have been compiled in Figures 7 to 9. Clearly, R245fa outperforms R410a

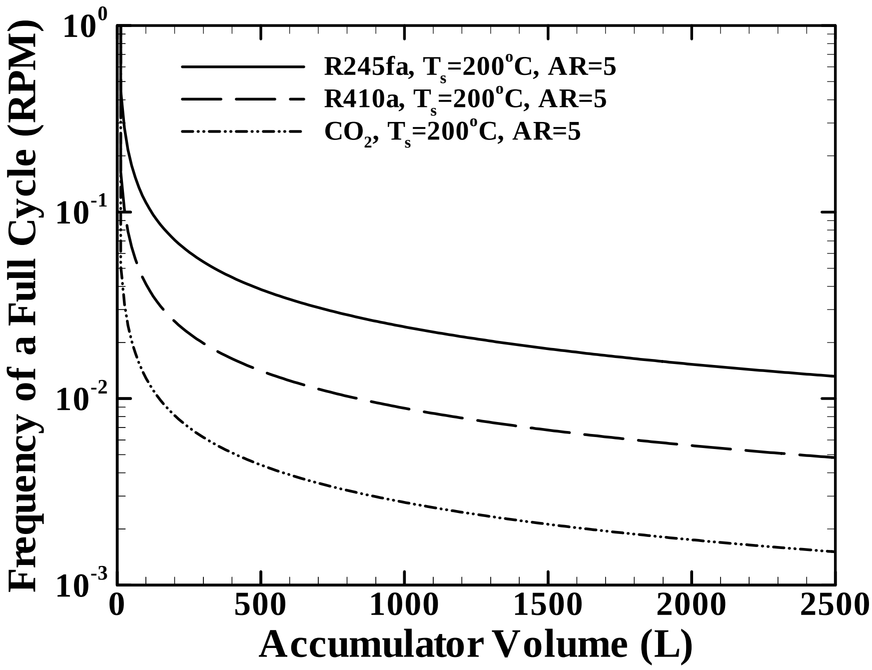

Figure 5: Frequency versus accumulator volume for R245fa, R410a and CO_2.

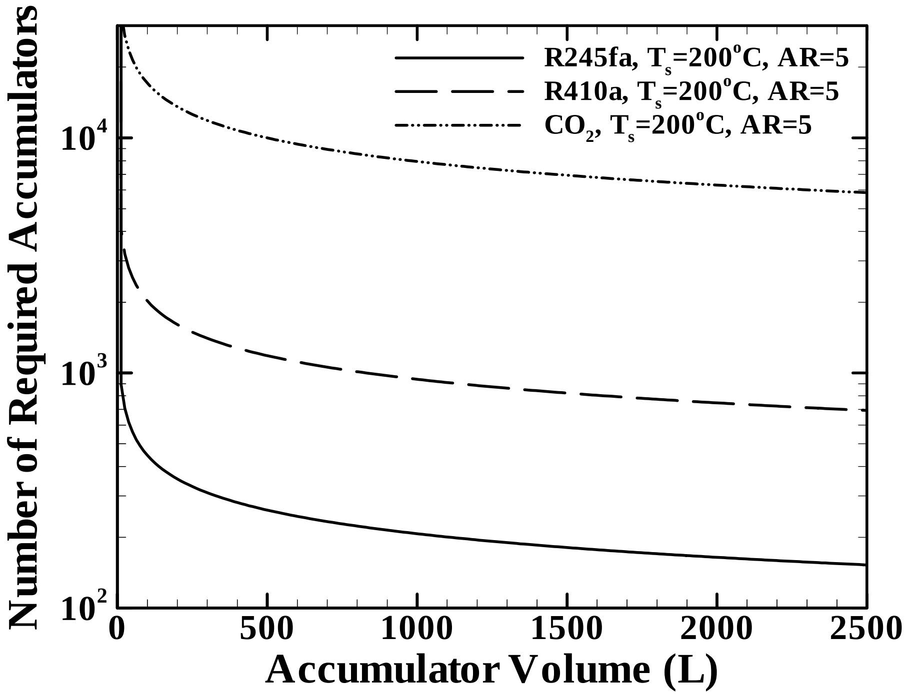

Figure 6: Number of required accumulators for 1 MW net power (R245fa, R410a and CO_2).

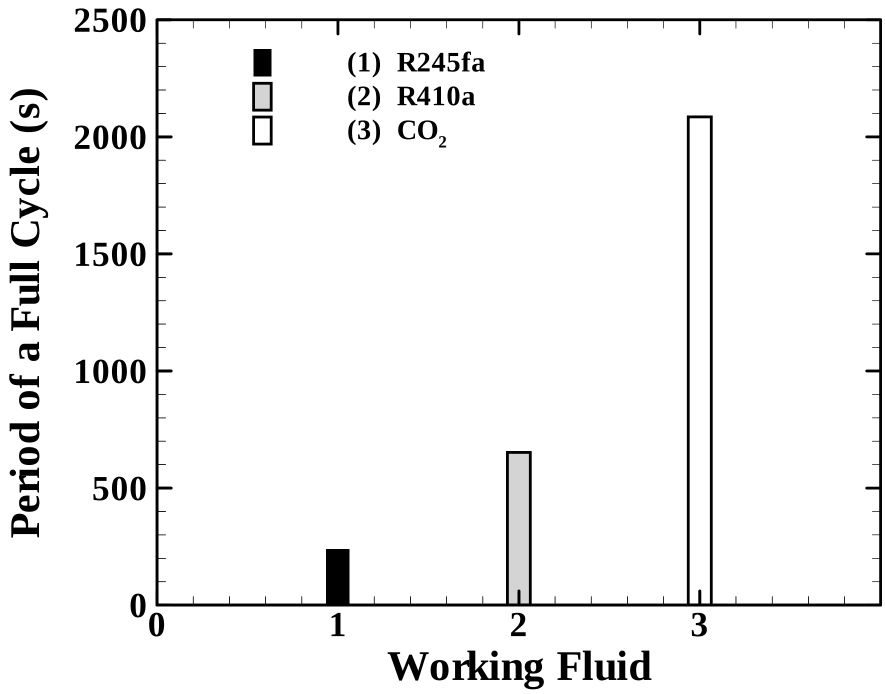

Figure 7: Comparison of cycle periods for a 30 L accumulator at a source temperature of 200^{o}C.

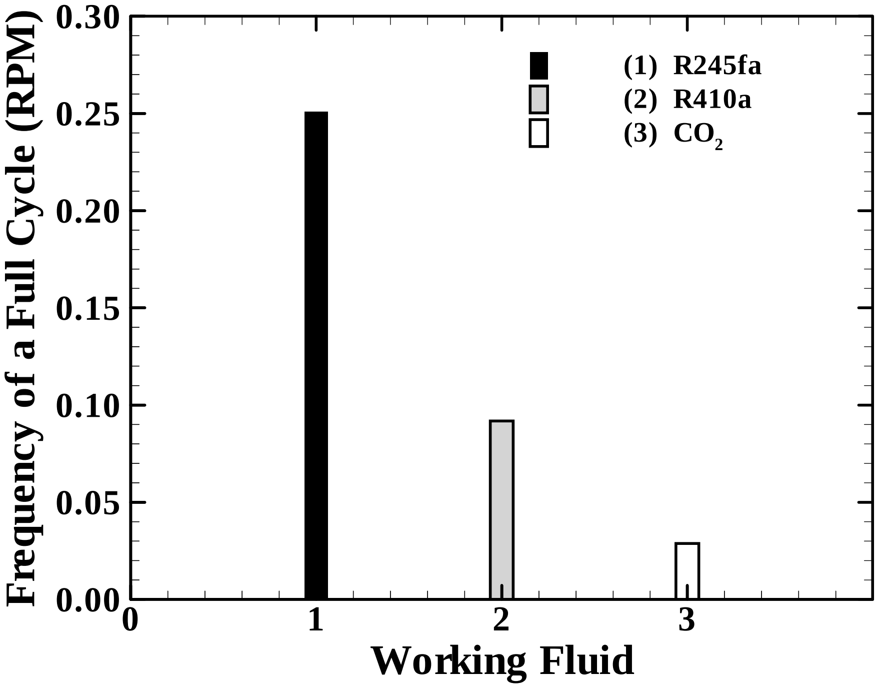

Figure 8: Comparison of cycle frequencies for a 30 L accumulator at a source temperature of 200°C.

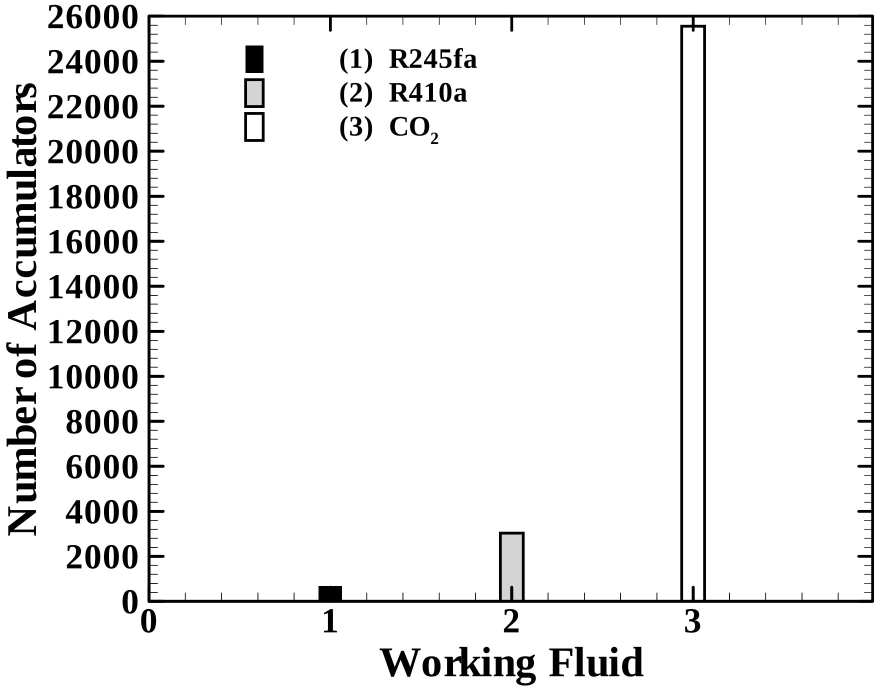

Figure 9: Comparison of accumulator numbers for a 30 L accumulator at a temperature of 200°C.

and CO_2 in terms of cycle period, cycle frequency and the required number of accumulator units. For example in the case of R245fa the cycle period for a 30 L accumulator unit is 239 s whereas those of the R410a and CO_2 are 652 s and 2085 s. The corresponding frequencies for R410a and CO_2 are approximately 0.1 RPM and 0.03 RPM while that of the R245fa is much higher at approximately 0.25 RPM. The greatest disparity among the three working fluids manifests itself in the number of accumulators with R245fa requiring 667 accumulator units of 30 L capacity whilst R410a and CO_2 require 3027 and 25553 units, respectively.

Figure 10 illustrates the thermal efficiency for R245fa, R410a and CO_2 at a source temperature of 200^{o}C. As noted earlier, the ambient temperatures used in the calculations associated with R245fa and R410a were all 25^{o}C while due to thermodynamic requirements an ambient temperature of 20^{o}C was considered for CO_2. As a bench-marking exercise the Carnot efficiency has also been included in Figure 10 for both 20^{o}C and 25^{o}C ambient temperatures.

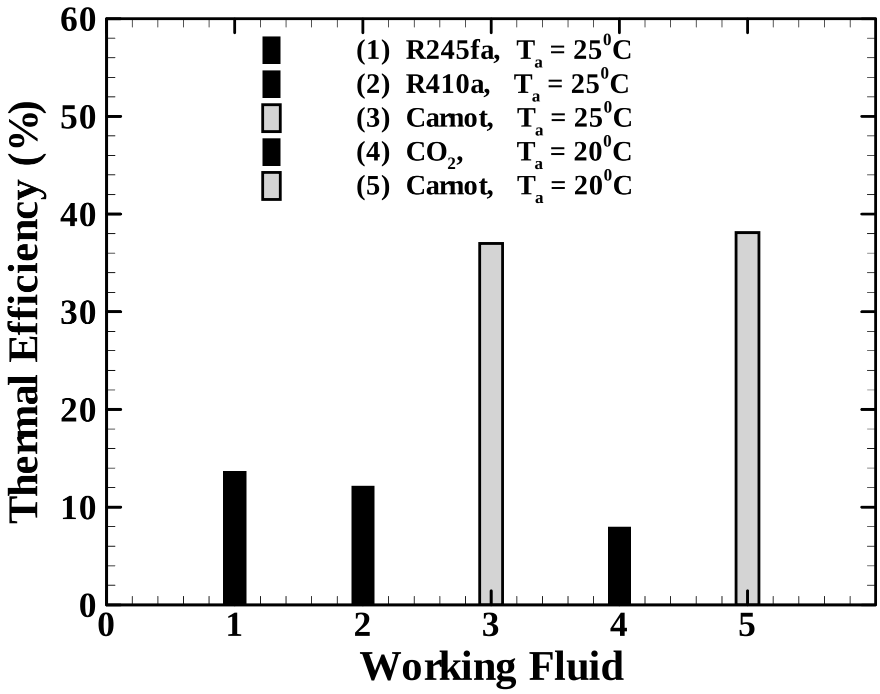

Figure 10: Comparison of thermal efficiency for a 30 L accumulator at a source temperature of 200^{o}C.

Under the operating conditions outlined above, R245fa attains a thermal efficiency of about 13.7% while R410a is 12.2% and CO_2 8%. The comparison of R245fa and R410a efficiencies with the Carnot efficiency at a 25^{o}C ambient (≈ 37%) reveals that in the case of R245fa, thermal efficiencies of up to 37% of the Carnot efficiency can be realised (that is: 13.7% / 37% = 37%). The above figure for R410a reduces to about 33% of the Carnot efficiency (that is 12.2% / 37% = 33%). A similar comparison between CO_2 and Carnot efficiency at the ambient temperature of 20^{o}C (≈ 38.1%) show that CO_2 can only reach 21% (i.e. 8% / 38.1% = 21%) of the maximum theoretical value defined by Carnot efficiency.

Plots of thermal efficiency and number of accumulator units against source temperature over a range between 120^{o}C and 200^{o}C (case studies 1-4, 11-14, 21-24) are shown in Figures 11 and 12, respectively. The results shown in these two figures have been calculated assuming a 30 L accumulator size with an aspect ratio of 5. As can be seen from Figure 11, the efficiency plot for R245fa gradually increases over the temperature range of 120^{o}C-150^{o}C, reaching a value of 11.4% at 150^{o}C. The efficiency plot for R245fa then plateaus reaching a maximum value of 13.7% at 200^{o}C. While a very similar trend is observed for R410a, the efficiency plot for CO_2 exhibit a much more linear profile particularly at source temperatures below 175^{o}C. Over the same range of source temperatures and depending on the ambient temperature the Carnot efficiency is 37% and 38.1%.

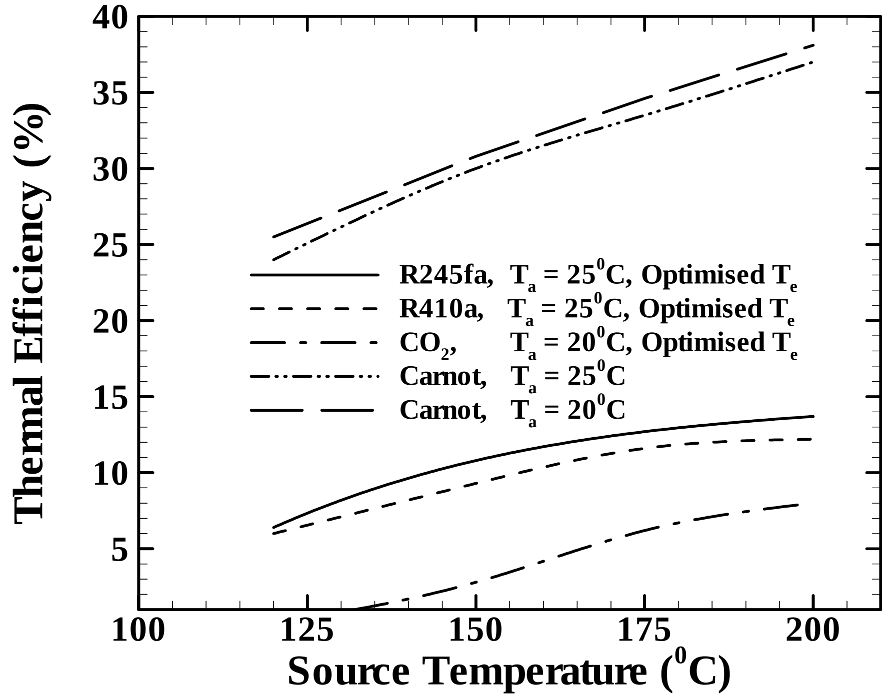

Figure 11: Plots of thermal efficiency against source temperature for R245fa, R410a, and CO_2.

It is interesting to note that while both R410a and CO_2 achieve higher maximum cycle pressures than R245fa (see Table 4), their performance characteristics in terms of cycle period, frequency, efficiency, and output power per accumulator unit are lower than those of R245fa. The thermodynamic explanation for this observation is that both R410a and CO_2 experience relatively high minimum cycle pressures (note: the minimum cycle pressures for R410a and CO_2 are 1.9 MPa and 6.5 MPa, respectively, whereas the minimum cycle pressure for R245fa is only 0.2 MPa, see Tables 1, 2, and 3). As a result, the expansion ratios (P_{max} / P_{min}) of R410a and CO_2 are much lower than those corresponding to R245fa. Given that the mechanical work (i.e. work generated during the sub-process 4 to 5 in Figure 2) and thereby the output power are directly proportional to expansion ratio then use of R410a and CO_2 as working fluids must lead to much lower output powers per accumulator unit.

A related observation from Table 4 is that the output power per accumulator unit for R245fa with a 30 L accumulator shows an increasing trend over the range of temperatures between 120^{o}C and 150^{o}C while a decreasing trend is observed for temperatures between 150^{o}C and 200^{o}C. This particular phenomenon is due to thermodynamic properties of R245fa and thermo-physical constrains imposed on the working fluid in Otello heat engine. Essentially, as the source temperature is raised from 120^{o}C to 200^{o}C, the pressure at point 2 and hence the required power for pump steadily rises (see Figure 2). The power generated due to expansion (i.e. work between points 4 to 5 in Figure 2) also increases as a result of increasing the source temperature but at a different rate. The net power output is a trade off between the expansion power and pumping power, and is defined as the difference between the two. At some point (for example temperatures greater than 150^{o}C for R245fa) the rise in the pumping power will inevitably overtake the corresponding rise in the expansion power, reducing the overall output power.

The above phenomenon also manifests itself in the minimum number of required accumulator units. As shown in Figure 12 the plots of accumulator numbers versus source temperature for both R245fa and R410a are nonlinear and have a minimum value. The minimum number of accumulator units for R245fa corresponds to a source temperature of 150^{o}C while in the case of R410 the minimum value corresponds to a source temperature of about 155^{o}C. The existence of these minimum points highlights that R245fa and R410a are more suitable for source temperatures between 150°C and 155°C despite the fact that slightly higher thermal efficiencies can be achieved at source temperatures around 200°C. In other words it can be concluded from Figures 11 and 12 that by sacrificing a small percentage of thermal efficiency and operating at a lower source temperature one needs a much smaller number of accumulator units to achieve a given power output. The number of accumulator units is a key parameter underpinning the capital cost of an Otello type heat engine.

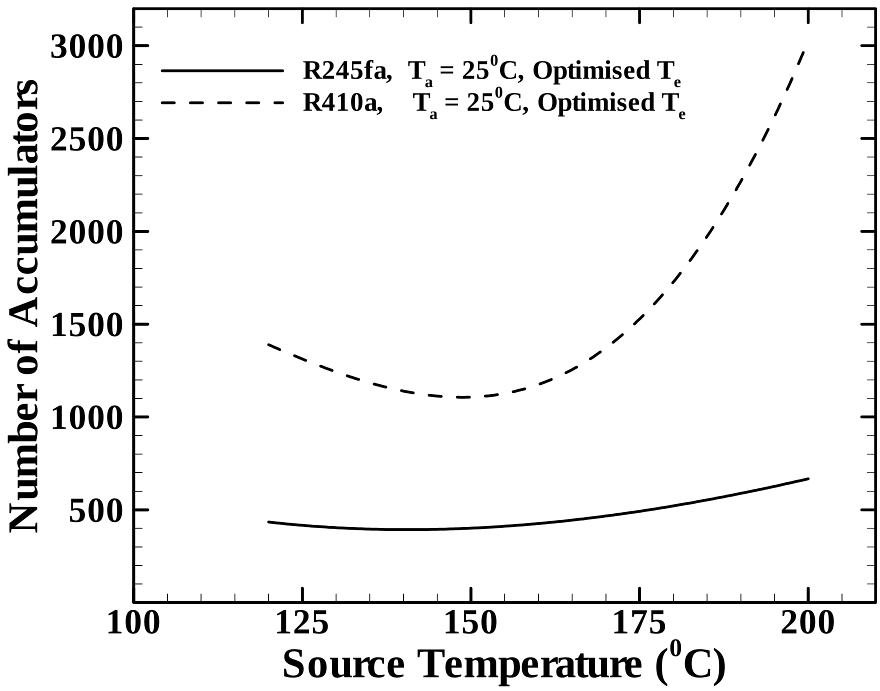

Figure 12: Plots of accumulator numbers against source temperature for R245fa, R410a, and CO_2.

4. CONCLUDING REMARKS AND RECOMMENDATIONS

The main conclusions from this study for accumulators with an aspect ratio of 5 are:

1. Of the three working fluids studied, R245fa is the most suitable working fluid for the Otello heat engine as it delivers the highest thermal efficiency and requires the lowest number of accumulator units for a given power output.

2. To generate 1 MW of power at a source temperature of 200^{o}C and an ambient temperature of 25^{o}C, R245fa requires 667 accumulators of 30 L capacity. The corresponding thermal efficiency is 13.7%.

3. To generate 1 MW of power at a source temperature of 150^{o}C and an ambient temperature of 25^{o}C, R245fa requires 401 accumulators of 30 L capacity. The corresponding thermal efficiency is 11.4%.

4. Considering remarks 2 and 3, it can be concluded that R245fa is more suited to source temperature around 150^{o}C despite lower thermal efficiencies because as the number of accumulators is significantly reduced the capital cost is significantly less.

5. As noted above, even at an optimum source temperature of 150^{o}C several hundred 30 L accumulators are needed to produce 1 MW of power. Issues associated with operation and maintenance of such a large number of unit operations have to be investigated in-depth.

6. The results and conclusions presented in this report are purely based on theoretical predictions and should be used only as a guide. Experiments should be carried out to verify the validity of modelling predictions given that simplified and/or conservative assumptions were made in developing the analysis tool, particularly with regards to heat exchange processes in the bath, overall heat losses from the engine, and the heat rejection process during working fluid condensation.

Appendix A: Interim Report

Discipline of Chemical Engineering
School of Engineering, Faculty of Engineering & Built Environment
The University of Newcastle, University Drive, Callaghan, NSW 2308, Australia

Technical Assessment of the Otello Heat Engine

PRELIMINARY REPORT

on

The Performance Characteristics of Otello Heat Engine Using R245fa Working Fluid

Prepared by:

Dr Elham Doroodchi
Prof Behdad Moghtaderi

Date: 7 Sept, 2009

Report Prepared for the International Innovation Limited (IIL)

Disclaimer
The conclusions presented in this report are based on a series of preliminary analysis and may change as the results of the complete set of analyses become available.

BACKGROUND

The University of Newcastle was sub-contracted in early 2009 to assess the technical feasibility of the Otello heat engine developed by the International Innovation Limited (IIL). The work plan comprised:

- Stage 1- Development of an analysis tool based on thermodynamic and heat transfer principles.
- Stage 2- Case studies for 1 MW Otello plant.
- Stage 3- Preparation and dissemination of milestone reports.

The scope of the technical assessment for case studies associated with Stage 2 was limited to:

- Working fluids: R245fa, R410a, and carbon dioxide (CO_2).
- Heat source temperature of 150^{o}C, 72^{o}C, and 31.5^{o}C.

SUMMARY

The preliminary report presented in this submission: (i) provides an overview of the analysis tool being developed by the University of Newcastle, UoN, for the Otello heat engine project, (ii) presents a preliminary assessment of the Otello heat engine and its performance characteristics when R245fa is used as the working fluid. As detailed in the following sections our preliminary thermodynamic analysis indicate that the Otello system in conjunction with R245fa can attain a thermal efficiency of 11.4% at 150^{o}C. At this temperature the Carnot efficiency which is the maximum theoretical thermal efficiency for any given thermodynamic power cycles is 30%.

OVERVIEW OF THE UNIVERSITY OF NEWCASTLE (UoN) ANALYSIS TOOL

Conceptual Framework of the UoN Analysis Tool

The development process for the UoN analysis tool initially began by examining the suitability of commercially available process simulation software packages such as HYSYS and CyclePad for modelling of the Otello heat engine. None of these commercial packages were found to be suitable and as such it was decided to develop a dedicated analysis tool for the Otello system which:

- Considers a fixed mass of the working fluid within the accumulator cylinder during major processes associated with the Otello thermodynamic cycle.
- Takes into account both thermodynamic and heat transfer issues.
- Robust enough to model both piston and bladder type accumulator cylinders systems.

The sub-processes considered in this study for the Otello heat engine thermodynamic cycle are schematically illustrated in Figure 1. The corresponding cycle on the temperature-entropy (T-S) diagram is also shown in Figure 2.

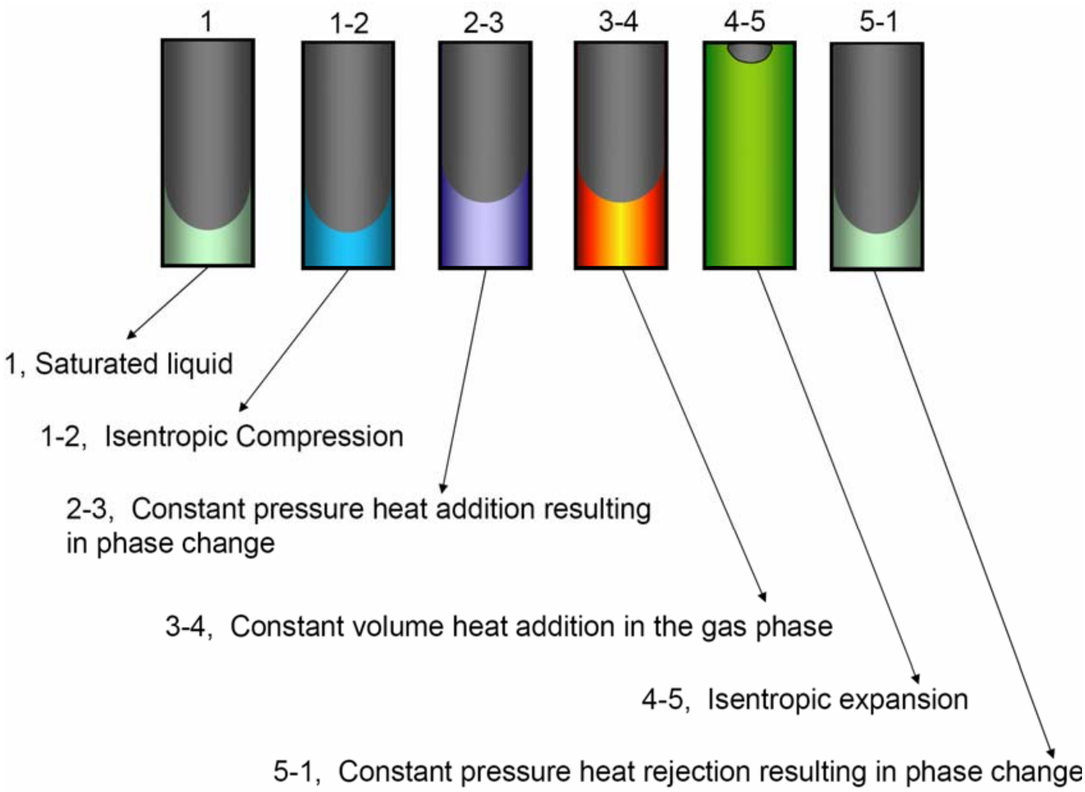

Figure 1: Schematic of the Otello heat engine sub-processes.

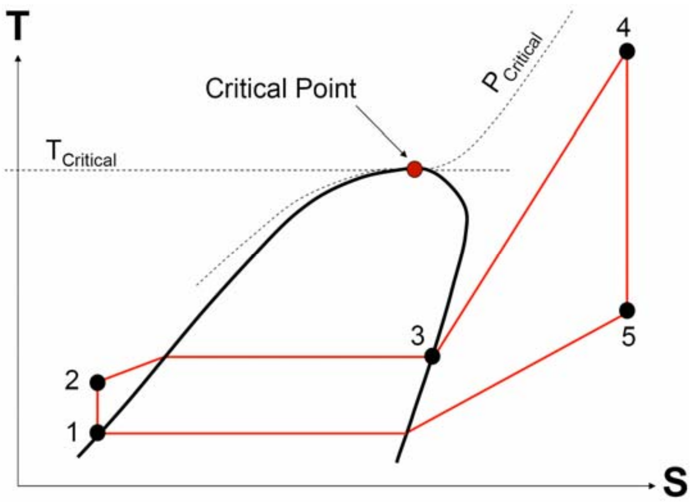

Figure 2: Schematic representation of the Otello heat engine on a T-S diagram.

As can be seen from Figures 1 and 2, the Otello thermodynamic cycle in the UoN model begins with pumping the working fluid from the saturated liquid State 1 to sub-cooled liquid State 2. The heat addition phase then commences. The energy added to the Otello system during the heat addition phase originates from a heat source. Rather than direct heat exchange between the source and the accumulator cylinder, the thermal energy of the source is used to heat up a bath of water or oil in which the accumulator cylinders are placed. The heat addition process initially takes place between States 2 and 3 under constant pressure where as shown in Figure 1 the working fluid experiences some slight expansion. Once the working fluid reaches the saturated vapour State 3 the heat addition process continues under constant volume. As a result, the pressure and temperature of the working fluid rise until it reaches its maximum temperature at the superheated State 4. The working fluid is then isentropically expanded to State 5. The volume of the working fluid during the expansion phase increases dramatically causing the piston (or bladder) to move, in turn, forcing the hydraulic liquid out of the accumulator generating mechanical work. Upon full expansion, the process of heat rejection to a cooling medium begins at constant pressure (between States 5 and 1) and the cycle comes to completion once the working fluid reaches State 1. The processes described above are then repeated. It should be noted that the T-S diagram shown in Figure 2 suggests that the Otello heat engine can be operated at temperatures higher than the critical temperature of the working fluid provided that the maximum cycle pressure is maintained at levels below the critical pressure.

In terms of the solution methodology the UoN analysis tool carries out two sets of simultaneous calculations, namely: (i) energy balance and (ii) heat transfer. While the total energy exchanged during a given cycle is determined through the energy balance calculations based on thermodynamic principles, heat transfer calculations allow the transient behaviour of the Otello heat engine to be uncovered. Essentially the heat transfer calculations can tell us how long it would take for the thermal energy of the heat source to be transported to the working fluid inside the accumulator cylinder. This, in turn, allows us to accurately determine the period of a full cycle, the frequency of the system (e.g. revolution per minute, RPM), and the required number of accumulator cylinders to achieve a desired power output. Other performance characteristics of the engine, such as the thermal efficiency and the net power output can be determined from the energy balance calculations. The energy balance for the accumulator cylinder in the UoN analysis tool is carried out by determining the internal energy, entropy, density, temperature and pressure of the working fluid at States 1 to 5. The heat transfer calculations are performed on the basis of the well known lumped parameter analysis.

Update on the Development of the UoN Analysis Tool

The progress towards developing the UoN analysis tool has been solid and the researchers involved with the project have been able to:

- Develop the majority of the modelling algorithms.
- Compile most of the necessary thermodynamic properties, particularly for R245fa, into a collection of correlations suitable for energy balance calculations (70% of the correlations for R410a, and CO_2 have also been developed).
- Develop and debug the first version of the analysis tool (UoN-V01) using a combination of the Microsoft Excel and Visual Basic programming.

RESULT AND DISCUSSION

Eight case studies were carried out as part of the present report (Table 1). Case studies 1 to 6 were dedicated to a source temperature of 150^{o}C but accumulator cylinders of different capacities. The case study 7 on the other hand focused on the performance characteristics of an optimum size accumulator cylinder (determined from case studies 1 to 6) over temperatures from 100^{o}C to 200^{o}C. The relationship between the source temperature and maximum pressure was examined in the case study 8.

Table 1: Details of case studies 1 to 8 and corresponding operational parameters.

Parameter	Case Studies							
	1	2	3	4	5	6	7	8
Net power output (MW)	1	1	1	1	1	1	1	1
Accumulator capacity (L)	125	500	750	1000	2000	2500	125	125
Accumulator Diameter (m)								
Configuration A	0.1575	0.2500	0.2862	0.3150	0.3969	0.4276		
Configuration B	0.3145	0.5000	0.5720	0.6300	0.7930	0.8545	0.3145	0.3145
Configuration C	0.4740	0.7500	0.8585	0.9450	1.1900	1.2820		
Configuration D	0.6300	1.0000	1.1430	1.2570	1.5850	1.7100		
Accumulator aspect ratio (height to diameter or H/D)								
Configuration A	40.76	40.76	40.76	40.76	40.76	40.76		
Configuration B	5.12	5.12	5.12	5.12	5.12	5.12	5.12	5.12
Configuration C	1.51	1.51	1.51	1.51	1.51	1.51		
Configuration D	0.64	0.64	0.64	0.64	0.64	0.64		
Source temperature (^{o}C)	150	150	150	150	150	150	100-200	150
Ambient temperature (^{o}C)	25	25	25	25	25	25	25	25
* T_{app} (^{o}C)	40	40	40	40	40	40	40	40
Volume Expansion (V_{max}/V_{min})	4	4	4	4	4	4	4	4
Minimum pressure (MPa)	0.2	0.2	0.2	0.2	0.2	0.2	0.2	0.2
* Re	40,000	40,000	40,000	40,000	40,000	40,000	40,000	40,000

* T_{app} ≡ Approach temperature between the water bath and the working fluid in accumulator cylinder
* Re ≡ Reynolds number of water flow in the bath. The flow is induced by stirring in an attempt to enhance heat transfer.

Figure 3 illustrates the plots of the period of a full cycle versus the aspect ratio (i.e. H/D or height to diameter ratio) of the accumulator for case studies 1 to 6 (see Table 1). As can be seen the predicted cycle periods for all cases are greater than 200 s at aspect ratios below 10. It is also evident that at any given aspect ratio the cycle period is directly proportional to the accumulator capacity. For example at H/D = 5.12 the cycle period for a 125 L accumulator is 216 s whereas that of the 2500 L accumulator is about 1597 s. The frequencies (in revolution per minute, RPM) corresponding to cycle periods shown in Figure 3 have been plotted against the aspect ratio of the accumulator cylinder in Figure 4 (note: the period and frequency in Figures 3 and 4 have been plotted on a logarithmic scale).

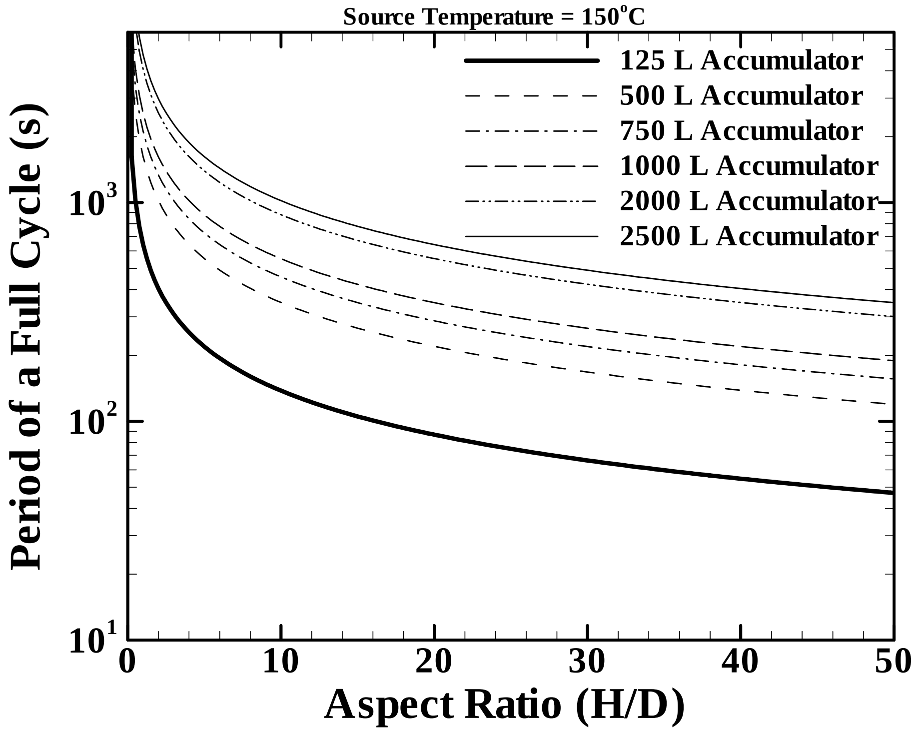

Figure 3: Cycle period versus accumulator aspect ratio for case studies 1-6.

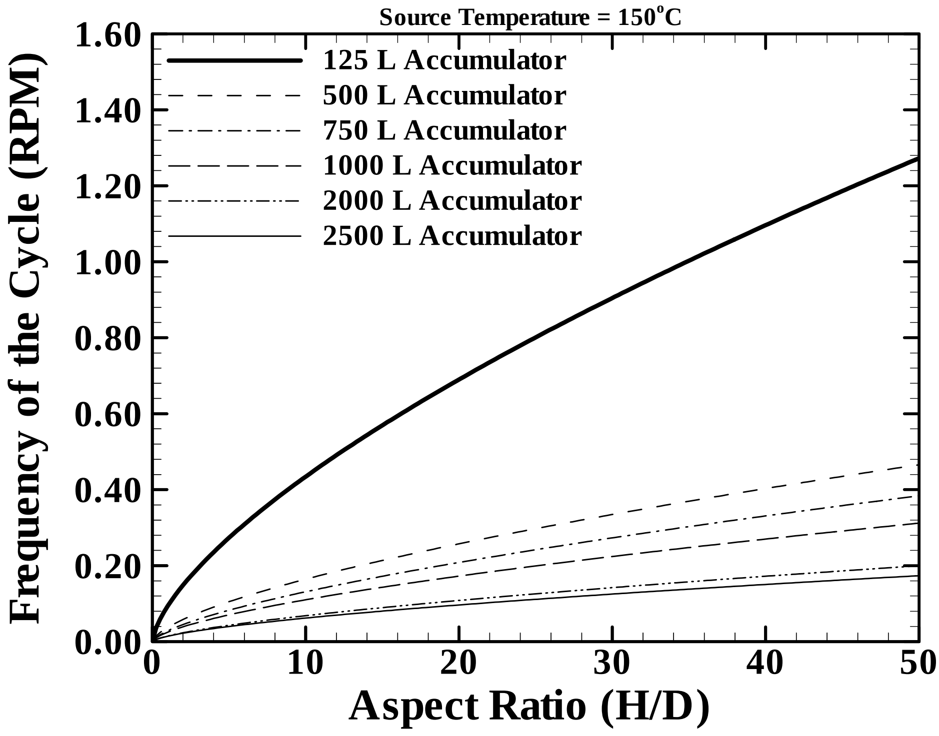

Figure 4: Frequency versus accumulator aspect ratio for case studies 1-6.

Figure 4 clearly demonstrates that for typical accumulator cylinders currently available in the market with aspect ratios below 10, the frequency is about half revolution per minute for an accumulator with a capacity of 125 L (see Figure 4). The frequency for larger capacity systems is typically lower than their small capacity counterparts. This reflects the large thermal inertia of the Otello system for temperatures associated with typical waste heat sources (i.e. 80°C to 160°C). Figure 5 shows the corresponding number of accumulators required to generate 1 MW of power for case studies 1 to 6. Like previous figures the accumulator numbers have been plotted against the aspect ratio.

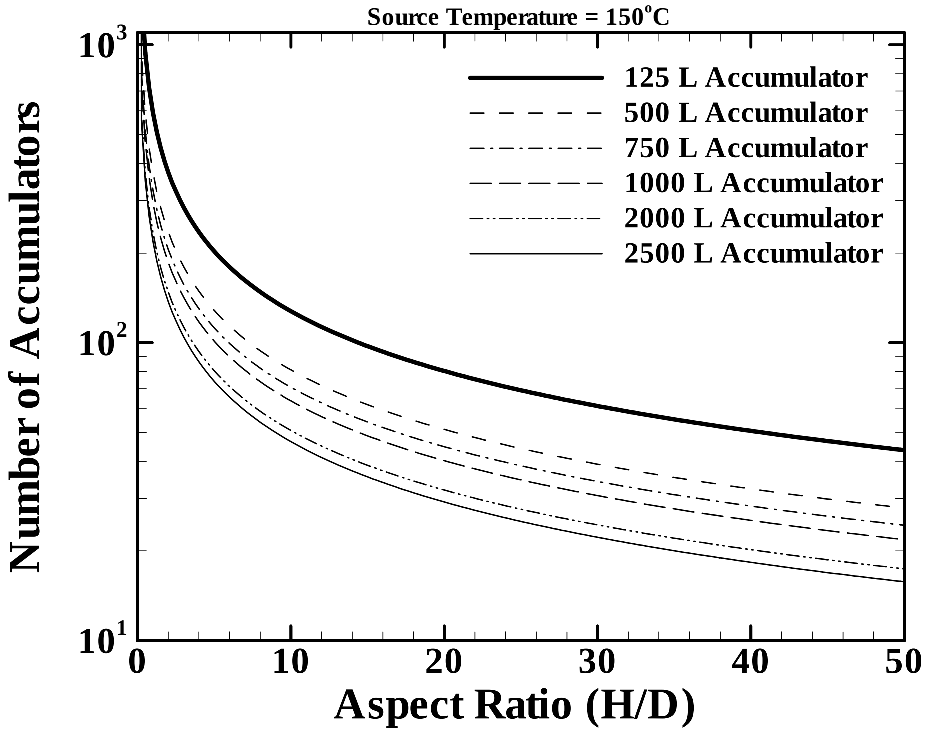

Figure 5: Number of required accumulators for a 1 MW net power output.

Interestingly, the combined volume of a large number of cylinders of small capacity (e.g. 125 L) is not necessarily bigger than those of a fewer number of medium (e.g. 1000 L) or large (e.g. 2500 L) accumulator cylinders. As shown in Figure 6 (points A, B, C, D, E, F) for an accumulator number of 300 the combined volume corresponding to: (A) 125 L is 28 m^3, (B) 500 L is 110 m^3, (C) 750 L is 165 m^3, (D) 1000 L is 220 m^3, (E) 2000 L is 441 m^3, and (F) 2500 L is 550 m^3. Therefore, from the point of view of equipment cost the use of a larger number of small capacity accumulator cylinders is more attractive than a smaller number or large capacity accumulators. For case studies 1 to 6 the most optimum combination turns out to be a system comprising 199 accumulators each with a capacity of 125 L and an aspect ratio of 5.12. The combined volume of the optimum system is 25 m^3.

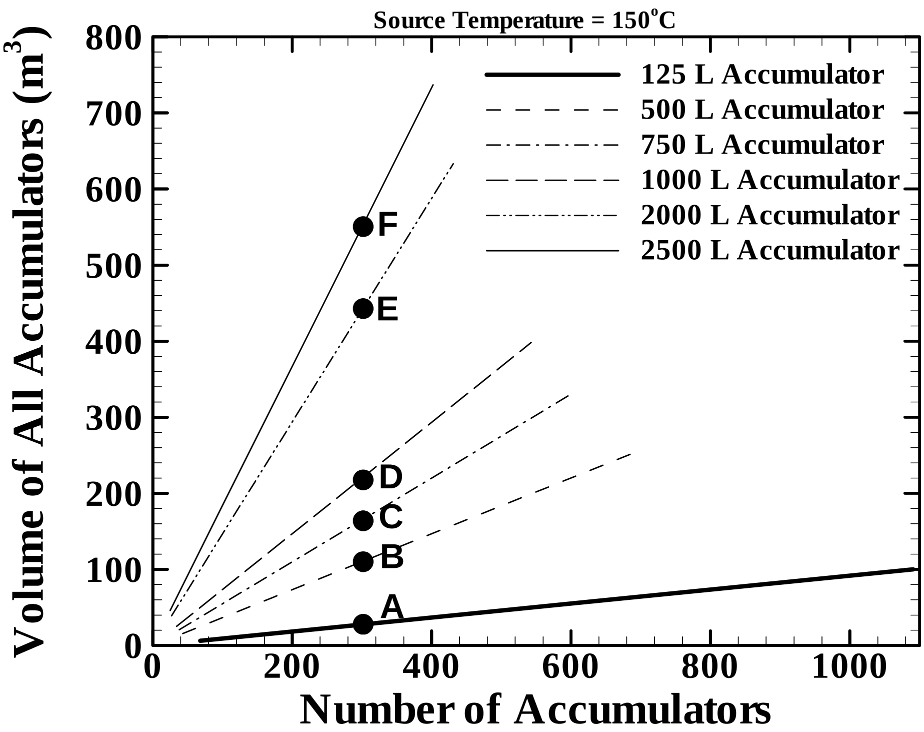

Figure 6: The volume of accumulators versus the number of accumulators required for 1 MW power.

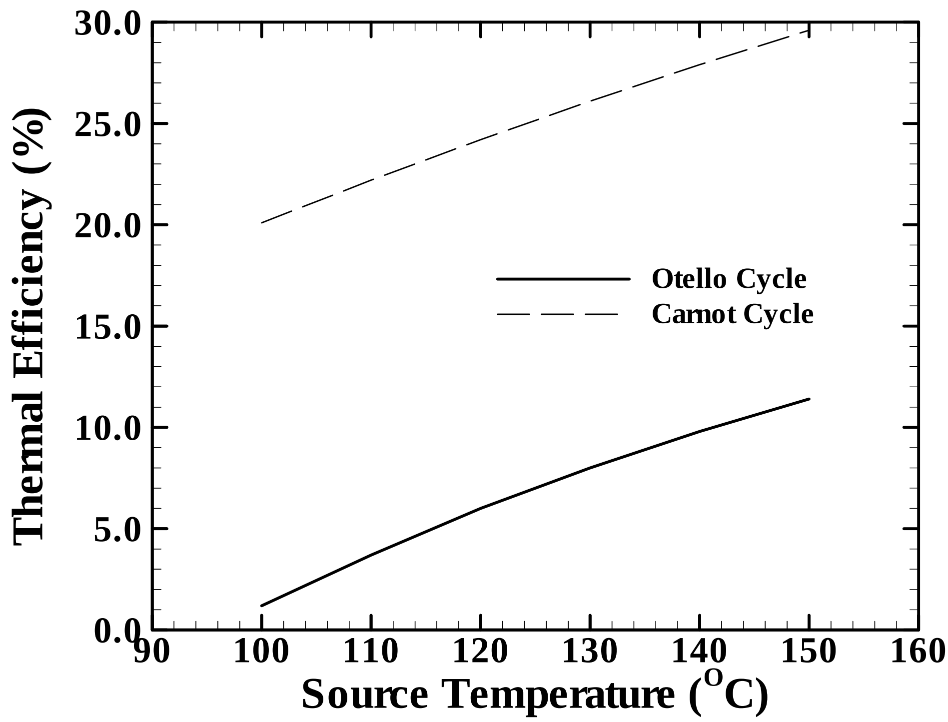

Figure 7: Plots of Otello and Carnot thermal efficiencies against the source temperature.

The optimum configuration identified in case studies 1 to 6 was selected for further analysis associated with case studies 7 and 8. Figure 7 illustrates the plot of thermal efficiency as a function of the source temperature for the optimum configuration outlined above. For comparison the Carnot efficiency has also been plotted. Carnot efficiency is a theoretical value which defines the upper limit (i.e. the maximum value) of thermal efficiency for a given set of source and ambient temperatures. As can be seen, the thermal efficiency of the Otello heat engine increases linearly reaching a value of 11.4% at 150^{o}C. Over the same temperature range the Carnot efficiency varies between 20% and 30% (i.e. an average efficiency of 25%).

One of the key thermodynamic characteristics of the Ottelo cycle is that the maximum cycle pressure (pressure at point 4 in Figure 2) is dependent on the rate of input thermal energy and the source temperature. As such, the maximum cycle pressure has to be calculated on the basis of thermodynamic constraints imposed by the first and second laws of thermodynamics and, hence, cannot be selected in isolation. Figure 8 shows the relationship between the source temperature and the maximum cycle pressure for the optimum system configuration outlined earlier in this report (i.e. case study 8). Clearly higher source temperatures lead to greater maximum cycle pressures. Our calculations indicate that at a source temperature of 150^{o}C, for instance, the cycle pressure increases to about 1.3 MPa. Higher pressures can only be achieved at higher source temperatures. For example according to our projections to attain a maximum cycle pressure of 3.2 MPa (32 bar) the source temperature should be about 190^{o}C (see Figure 8).

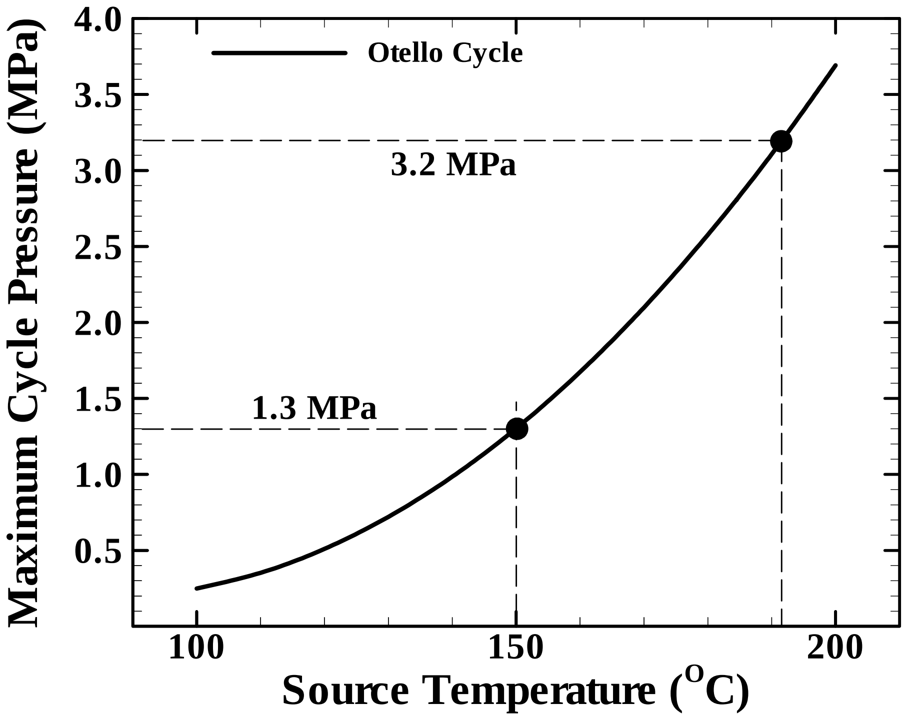

Figure 8: Plot of maximum cycle pressure versus source temperature.

CONCLUDING REMARKS

The main conclusions from this preliminary report are:

- For a nominal source temperature of 150^{o}C the Otello heat engine delivers a thermal efficiency of 11.4% which is about 37% of the Carnot efficiency for the same source temperature.

- For a source temperature of 150^{o}C and a target output of 1 MW, the optimum Otello system comprises 199 accumulator cylinders each with a capacity of 125 L and an aspect ratio of 5.12.

Our findings so far are limited to case studies associated with R245fa. More definitive and general conclusions can be drawn once the analyses on R410a and carbon dioxide are completed.

Appendix B: Additional Case Studies Requested by IIL

Table B1: Additional case studies requested by IIL for R245fa

Parameter	Case Studies (R245fa)								
	1	**2**	**3**	**4**	**5**	**6**	**7**	**8**	**9**
Net power output (MW)	1	1	1	1	1	1	1	1	1
Accumulator capacity (L)	30	30	30	125	500	750	1000	2000	2500
Accumulator Diameter (mm)	62	62	160	235	350	350	360	510	580
Accumulator aspect ratio (H/D)	160	160	9.3	12.3	14.9	22.3	27.3	19.2	16.3
Volume Expansion (V_{max}/V_{min})	4	4	4	4	4	4	4	4	4
Source temperature (^{o}C)	150	200	200	200	200	200	200	200	200
Ambient temperature (^{o}C)	25	25	25	25	25	25	25	25	25
Minimum pressure (MPa)	0.2	0.2	0.2	0.2	0.2	0.2	0.2	0.2	0.2
Number of accumulators	41	67	447	231	128	86	68	68	70
Thermal efficiency (%)	10.7	13.7	13.7	13.7	13.7	13.7	13.7	13.7	13.7
* Re = 40,000	✓	✓	✓	✓	✓	✓	✓	✓	✓

** Re ≡ Reynolds number of the heat transfer medium (e.g. water, thermal oil, etc) in the bath.*